APPLICATIONS OF
MODELLING AND SIMULATION
http://arqiipubl.com/ams eISSN 2600-8084 VOL 9, 2025, 164-173

Applicability of Static Analysis for Fracture Characterization of 3D Elliptical Disc Crack Under Dynamic Impact Loading

Sun Zhufeng[1,2], Inzarulfaisham Abd Rahim[1], Ooi Lu Ean[1] and Norwahida Yusoff[1*]

[1]School of Mechanical Engineering, Universiti Sains Malaysia, 14300 Nibong Tebal, Penang, Malaysia
[2]Academic Journal Center, Beijing Institute of Technology, 100081 Beijing, China

[*]Corresponding author: menorwahida@usm.my

Submitted 30 October 2024; Revised 27 March 2025; Accepted 18 April 2025; Available online 09 May 2025.

Abstract: Engineering and industrial structures, such as pressure vessels, power plants, and offshore platforms, may develop defects like cracks and corrosion during manufacturing and service life. These defects significantly affect the dynamic load response of the structure, complicating the prediction of the structure's carrying capacity and the accuracy of risk assessments. Due to this complexity, characterizing the dynamic stress intensity factor is challenging. Therefore, it is necessary to understand the dynamic response of defective structures. This study aims to analyze the dynamic fracture mechanics of a buried three-dimensional elliptical disc crack using finite element analysis by examining the stress response under dynamic impact loads. The influence of the crack geometry of the elliptical disc crack on the structural strength of different materials; aluminum alloy, stainless steel and cast iron, was further examined and compared with static analysis. The results of finite element analysis show that under impact load, when the elliptical disc crack is relatively small and the structure's dimension can be considered infinitely large, the crack geometry noticeably affects the stress distribution and stress magnitude the crack tip, which is consistent with the mathematical deduction. Under the same dynamic loading and crack geometry conditions, brittle cast iron is more sensitive to dynamic impact than stainless steel and aluminum alloy, with stress magnitudes in cast iron also a little higher than those in the other two materials. Stress analysis of the crack tip further reveals that the distribution of stress field under impact load is similar to that under static load, and the maximum principal stress under dynamic impact load is lower than that under static load for all three materials. Based on these findings, the static maximum principal stress analysis can sufficiently be used to characterize fracture properties of three-dimensional cracked bodies under dynamic impact loading and reduce the workload associated with the dynamic analysis.

Keywords: Dynamic stress intensity factor; Dynamic fracture toughness; Elliptical disc crack; Fracture mechanics; Impact load.

1. INTRODUCTION

Modern fracture mechanics originated from Griffith's classical fracture theory, which was later expanded by Irwin, who followed the mathematical sharp crack model and proposed the stress intensity factor (SIF) theory. The singularity theory, stemming from these early developments, continues to influence fracture mechanics today. However, there are fundamental contradictions within the singularity theory, both in its theoretical framework and methods. In engineering practice, the crack tip's curvature radius is not zero, and the stress-strain at the crack front is finite, meaning there is no stress singularity. Theoretically, the stress at the crack front approaches infinity, suggesting that no matter how small the crack or load, material failure would occur, which is an outcome that clearly differs from real-world observations. Improving the mathematical sharp crack model remains challenging, leading researchers to attempt modifications to the singularity theory to better align with experimental findings. For example, approaches have been explored and sought to establish fracture criteria based on stress parameters [1]. Based on the inevitable blunting of the crack tip and the finite nature of stress and strain, it has been demonstrated that the fundamental criterion for crack extension is either the maximum shear stress criterion (for ductile fracture) or the maximum principal stress criterion (for cleavage fracture), as shown through the analysis of three sets of experimental data. Under specific conditions, critical relations can be deduced [2]. Various fracture theories, such as the maximum tensile stress criterion for brittle failure and the maximum shear stress theory for ductile failure, have also been proposed [3]. Efforts to determine the stress field at the crack tip and unify the crack extension criterion with the stress intensity criterion represent key objectives for fracture mechanics researchers. Adibaskoro et al. proposed a method for simulating

multiple discrete crack propagations using the material point method (MPM). This approach dynamically allocates particles to different grids to simulate the extension behavior of multiple crack-paths and introduces an evaluation method for crack initiation and propagation based on the Rankine criterion. The study validated the effectiveness of this method by successfully simulating crack initiation, propagation, coalescence, and fracture processes [4].

For dynamic fracture mechanics, the challenge is compounded by the inertial effects of materials. The dynamic fracture criterion is used to determine specific dynamic fracture phenomena, including criteria for the initiation and unstable propagation of cracks under dynamic loading conditions, as well as bifurcation judgments for rapidly propagating cracks. The American Society for Testing and Materials (ASTM) and other organizations have published test methods for dynamic fracture toughness parameters $K_{Id}(\dot{\sigma})$ and $K_{Id}(V)$, which serve as important indicators for evaluating the ability of materials to resist crack propagation under dynamic loading conditions, and ensuring the safety and reliability of materials in high-speed impact environments. Here $\dot{\sigma}$ represents the rate of stress change under impact loading, and V is the speed of crack propagation. These are still considered reference protocols rather than standard testing specifications. Some researchers have discussed stress intensity factors for half-elliptical or elliptical cracks, but these theoretical solutions often fall short in practical engineering applications [5].

Several studies have compared static and dynamic fracture analysis. With this procedure, it was possible to compute dynamic fracture toughness [6]. The method demonstrates that measuring dynamic fracture toughness can be achieved without the need for crack sensors or strain gauges. It was observed that the fracture toughness of this steel under both static and dynamic conditions is quite similar, likely because this hardened steel exhibits very low strain rate sensitivity, meaning its dynamic and static properties do not differ significantly. This is because, when a static crack begins to propagate, the crack front is not idealized as a sharp crack and requires more resistance to advance. In contrast, during dynamic crack propagation, the crack front approaches the ideal sharp crack, resulting in reduced resistance.

Since the rise of fracture mechanics, significant progress has been made in understanding three-dimensional (3D) crack problems, but analytical calculations remain quite complicated. Researchers have been studying the behavior and mechanism of 3D cracks from various aspects. Nabavi et al. investigated the dynamic stress intensity factors (DSIFs) of longitudinal semi-elliptical cracks in thick-walled cylinders using the finite Hankel transformation and the three-dimensional finite element method. They derived the DSIFs at the deepest and surface points of the crack and found that dynamic loading causes fluctuations in the stress intensity factor. Their results also indicate that crack geometry, particularly the aspect ratio, significantly influences DSIF behavior. For narrow cracks, the deepest point consistently serves as the initiation site for crack propagation. However, for cracks with a large aspect ratio, the critical point along the crack front shifts between the deepest and surface points [7]. In general, the theory for 3D problems is far less mature than that for two-dimensional (2D) plane problems. Solutions for 3D crack problems are typically limited to simple force and boundary conditions, such as the infinite statics of a general disc crack under axisymmetric force and the dynamics of a disc crack under impact load. The static loading form of typical buried 3D elliptical disc cracks has been well studied [8]. However, because materials and structures are often subjected to dynamic loadings, it is more important to study elliptical disc cracks under these conditions, which are much more difficult to assess than under static loadings. He et al. proposed high-order smooth elliptical crack elements for simulating the stress intensity factor and T-stress of internal flat elliptical cracks. This method eliminates the node artifacts of traditional low-order elements by using high-order shape functions and Lagrange interpolation in radial and hyperbolic directions. Their approach successfully calculates crack opening displacements and stress intensity factors under various loading conditions [9].

Material properties and crack geometry are critical factors influencing crack propagation behavior, particularly under dynamic loading conditions. Different materials exhibit varying responses to dynamic loads. For instance, high-strength steel has lower strain rate sensitivity, maintaining stable mechanical properties across different loading rates. This results in more controllable stress distributions at the crack tip and a more stable crack propagation path. In contrast, aluminum alloys are more sensitive to loading rates, leading to pronounced changes in the stress field under dynamic loading and more complex crack propagation behavior [10]. Beyond material properties, crack geometry, particularly aspect ratio, plays a crucial role in determining crack propagation behavior. In elongated cracks, the deepest part typically serves as the initiation point, whereas in near-circular cracks, propagation may begin either at the deepest part or the surface. Research shows that the length-to-depth ratio strongly influences the stress intensity factor distribution at the crack front, especially under dynamic loading [11]. Therefore, analyzing the stress fields of three-dimensional cracks with varying geometric parameters across different engineering materials is crucial for evaluating structural integrity in engineering structures.

To investigate these effects, the present study employs finite element analysis using ANSYS and LS-DYNA numerical simulations to characterize dynamic stress fields. An engineering connection component is analyzed under the assumption that it contains internal defects, simplified as an elliptical disc crack. Considering the potential impact of transient tensile loading, the effect of occasional dynamic loads on the component is examined. The time history of the maximum dynamic principal stress at the crack front is computed and compared with the maximum principal stress under static loading to evaluate their correlation and assess the validity of using static analysis for fracture characterization. This comparison enhances the understanding of stress distribution and the extent to which static analysis can approximate dynamic conditions, offering a potential simplification for engineering assessments.

2. MATHEMATICAL DESCRIPTION OF THE PROBLEM

Figure 1 shows an elliptical disc crack in an infinite 3D elastic medium. Let the crack be in the $x_1 - x_2$ plane, and its normal direction coincides with x_3 direction, where $x_3 = 0^+$ and $x_3 = 0^-$ represent the upper and lower surface of the crack, respectively. $(x_1, x_2) \in \Omega$, where Ω represents the crack region, and a and b are the long and short half axes of the ellipse, respectively.

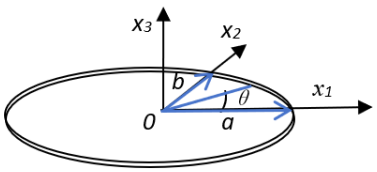

Figure 1. An elliptical disc crack.

Table 1. Material parameters, c_1 and c_2, for three different materials at 20 °C [12].

Parameter	Aluminum alloy	Stainless steel	Cast iron
c_1 (m/s)	6320	5940	4500
c_2 (m/s)	3100	3220	2440

Considering the parametric equation of the ellipse, the 3D elliptical crack at infinity is:

$$\frac{x_1^2}{a^2}+\frac{x_2^2}{b^2}\le 1 \tag{1}$$

and according to the Saint-Venant principle, the stress component σ_{ij} is:

$$\sigma_{33}=p_0 f(t),\ \ \sigma_{31}=\sigma_{32}=0 \tag{2}$$

where p_o is a constant representing a uniform stretch, σ_{33} is the normal stress in x_3 direction, and $f(t)$ is an arbitrary function of time. Because of x_1-x_2 planar symmetry, the study focuses on the half-space ($x_3>0$, or $x_3<0$). At this time, it can be assumed that there is an infinite force and compression stress on the crack surface. The initial boundary conditions for this problem in the half-space are:

$$\left.\begin{aligned} &u_i(x_1,x_2,x_3,0)=0\\ &\frac{\partial u_i(x_1,x_2,x_3,t)}{\partial t}|_{t=0}=0 \end{aligned}\right\} \tag{3}$$

$$\left.\begin{aligned} &\sqrt{x_1^2+x_2^2+x_3^2}\to\infty \ :\quad \sigma_{ij}=0\\ &x_3=0,\quad (x_1,x_2)\in\Omega \ :\quad \sigma_{33}=-p_0 f(t),\ \sigma_{31}=\sigma_{32}=0\\ &x_3=0,\quad (x_1,x_2)\notin\Omega \ :\quad u_3=0,\ \sigma_{31}=\sigma_{32}=0 \end{aligned}\right\} \tag{4}$$

Here u_i represents the displacement component, and the corresponding displacement field is given by:

$$\vec{u}=\nabla\Phi+\nabla\times\vec{\Psi} \tag{5}$$

where Φ is the Lame potential and Ψ is the Vector potential. This problem is solved by the wave control equations expressed as:

$$\nabla^2\Phi=\frac{1}{c_1^2}\frac{\partial^2\Phi}{\partial t^2}\ ,\qquad \nabla^2\Psi=\frac{1}{c_2^2}\frac{\partial^2\Psi}{\partial t^2} \tag{6}$$

where c_1 and c_2 are the longitudinal and transverse wave velocities, respectively. Table 1 shows the values of these velocities for three different materials at 20 °C.

The 3D crack dynamics problem is solved using partial differential equations with the initial conditions given in Equation (3) and the boundary conditions given in Equation (4). After applying the Laplace transformation and the double Fourier transformation to the system of Equation (6), Fan provides an integral representation method to get the displacement field solutions of impact load [12]. Let the load function $f(t)$ be the Heaviside function to represent the impact load:

$$f(t)=H(t)=\begin{cases}0\ , & t<0\\ 1\ , & t\ge 0\end{cases} \tag{7}$$

If the medial distance at the leading edge of the crack is ε, the crack opening displacement in the Laplace transform domain (s domain) is replaced by $u_3^*(x_1,x_2,0,s)=u_3^*(\varepsilon,\theta,0,s)$, where u_3^* is the Laplace transform of physical space displacement u_3 along the x_3 direction. Since the position of the point is given by the angle $\theta=\arctan(x_2/x_1)$, then:

$$u_3^*(\varepsilon,\theta,0,s)=\frac{2(1-\nu^2)}{E\sqrt{\pi}}(2\varepsilon)^{1/2}K_{\mathrm{I}}^*(b/a\ ,\theta,s) \tag{8}$$

Equation (8) reveals the relationship between the crack opening displacement and the mode I stress intensity factor, where E is the elastic modulus, ν is the Poisson ratio, and K_{I}^* is the mode I stress intensity factor in the Laplace transform domain (s domain) given by:

$$K_{\mathrm{I}}^{*}(b/a,\theta,s)=\lim_{r\to 0}\sqrt{2\pi r}\,\sigma_{33}^{*}(x_1,x_2,0,s) \tag{9}$$

Here σ_{33}^{*} is the Laplace transform of physical space stress σ_{33} along the x_3 direction, the stress intensity factor can also be obtained by taking the extreme value $\varepsilon \to 0$ of Equation (8) and is more accurate when calculated using displacement rather than stress. In Equation (8), the stress state at the leading edge of the crack is plane strain. After obtaining $K_{\mathrm{I}}^{*}(b/a,\theta,s)$ from Equation (8), the Laplace inversion of the transformation is performed, i.e.:

$$K_{\mathrm{I}}(b/a,\theta,s)=L^{-1}\left(K_{\mathrm{I}}^{*}(b/a,\theta,s)\right) \tag{10}$$

This allows for obtaining the stress intensity factor in the physical time-space domain. Clearly, in addition to the external stress, p_o, and $f(t)$, and the Poisson's ratio, v, the factor is also related to geometric parameters b/a and the angular parameter, θ. The results indicate that when comparing the dynamic stress intensity factor with that of static 3D elliptical disc cracks, a smaller b/a ratio results in larger $K_{\mathrm{I}}(t)_{max}$ values, which is consistent with the behavior of static cracks. In reference [10], $K_{\mathrm{I}}(t)_{max}$ /K_{I} is less than 1.0, where K_{I} is static stress intensity factor. K_{I} can also compare with the Green-Sneddon solution [13] for the elliptical disc crack problem under uniform tension:

$$K_{\mathrm{I}}=\frac{P_0\sqrt{\pi}}{E(k)}\left(\frac{b}{a}\right)^{1/2}(a^2\sin^2\theta+b^2\cos^2\theta)^{1/2} \tag{11}$$

where $E(k)$ is the complete elliptic integral of the second kind, $k^2=(a^2-b^2)/a^2$. According to the Green-Sneddon solution, when b/a = 0.5, K_{I} is 0.88. The analyzed solution is derived based on several mathematics assumptions; hence it does not perfectly coincide with experimental results.

This mathematical analysis demonstrates that even for a simple kinetic problem, the analytical solution relies on numerous assumptions. As a result, the validity of these solutions often does not align with experimental outcomes. While some assumptions are partially addressed through dimensional analysis in calculations, making the numerical solutions somewhat useful as references, the differences between the assumptions of the analytical solutions and actual load conditions, combined with the difficulty of solving complex load scenarios, have led to a growing reliance on a combination of finite element methods and experimental approaches to address practical problems. Consequently, there has been limited progress in fracture mechanics and fracture dynamics over the past two decades. Therefore, this study aims to numerically analyze the stress field distribution of a buried elliptical disc crack in a finite structure made of aluminum alloy, stainless steel, and cast iron under both dynamic impact and static loads. The study will compare the principal stress at the crack front for different materials and crack geometry ratios, b/a, under these loading conditions.

3. FINITE ELEMENT ANALYSIS

3.1 Finite Element Model

The static analysis was carried out using the commercial finite element analysis software ANSYS, while LS-DYNA was used for the analysis of dynamic stress intensity under impact load. When establishing a finite element model, the infinite crack is approximated by a finite-size cylinder. If the cylinder's diameter is significantly larger than the long axis of the buried elliptical disc, this setup effectively simulates in an infinite dimension. The simulated crack model is shown in Figure 2. The cylinder has a height, H, of 80 mm and a diameter, d, of 320 mm, with a buried elliptical disc crack located at its center. The long half-axis of the crack is a = 8 mm. To study how the shape of the elliptical disc crack responds to impact loading, the short-axis radius, b, is varied at 2 mm, 4 mm, and 6 mm. The static tensile stress is p = 1 MPa, while the impact load tensile stress is p = 1 × $H(t)$ MPa, and the $H(t)$ in this paper is set as Heviside fuction. Due to symmetry, only half of the cylinder is analyzed. Both dynamic and static finite element analyses use the same boundary conditions: the bottom surface of the cylinder is fixed, and the load is applied to the top surface.

For the boundary and load analysis setup, the symmetry of the structure and loads was considered. The displacement in the x-direction was constrained to zero on the symmetry plane. Load was applied on the top surface of the structure, while the bottom surface was fixed. The model was constructed using ANSYS's predefined fracture model with the semi-elliptical crack module. Tetrahedral elements were applied at the crack tip to capture its singular behavior, and an adaptive meshing method was employed to refine the mesh near the crack tip, with density gradually decreasing farther away. The patch-conforming algorithm was used with a second-order polynomial. To ensure accuracy, a mesh convergence analysis confirmed that further refinement did not affect the results, validating the adequacy of the mesh and the accuracy of the finite element analysis.

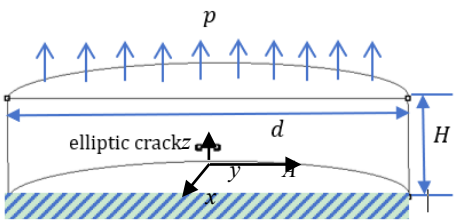

Figure 2. A three-dimensional elliptical disc crack.

3.2 Static Analysis

The stress intensity factor of the elliptical disc crack under static loading was analyzed using ANSYS. For comparison with the theoretical solution, the characteristic size of the elliptical disc crack is more than 20 times larger, allowing it to be considered as a buried elliptical disc crack in an infinite medium. The crack length ratios of the elliptical disc are b/a = 0.25, 0.5, and 0.75, with a static load of p = 1 MPa applied in each case. The materials under examination are aluminum alloy, stainless steel, and cast iron, with their mechanical properties detailed in Table 2.

The maximum principal stress, σ_{1max}, at various positions along the leading edge of the elliptical disc crack is presented in Table 3. The results show that the stress fields vary with different materials, and the crack shape ratio of the elliptical disc crack, b/a, significantly influences the stress response at various angular positions on the crack's front edge. Additionally, when b/a = 0.25, the ratio of $\sigma_{1\max}$ at 90 and 0 is 1.7. When b/a = 0.5, the ratio is 1.284, and when b/a = 0.75, the ratio is 0.99. This indicates that a smaller b/a ratio leads to a more even distribution of stress along the crack's front edge and results in lower maximum stress values $\sigma_{1\max}$.

The influence of geometric and material parameters is further examined by analyzing K_1 and the maximum principal stress, σ_{1max} distribution along the crack front for the three materials under the same loading and boundary conditions, as shown in Figures 3 and 4, respectively. The mesh nodes are also displayed along the crack front in the model. Figure 3 shows that K_1 varies slightly with different materials but is significantly influenced by the crack shape. This finding is consistent with the Green-Sneddon solution [13], although the values do not match exactly.

Similarly, Figure 4 demonstrates that under the same load, σ_{1max} is influenced by both the geometric parameters of the crack and the material. However, the material has a lesser impact, while the crack shape plays a more significant role. A similar pattern is observed for the principal stress. It should be noted that researchers typically select the geometric shape parameter b/a and the position parameter (angle) as key analytical parameters [14-16]. However, for elliptical disc cracks, the crack perimeter is also a crucial factor influencing the stress field distribution at the crack front. When the major axis of the elliptical crack is fixed, varying b/a by adjusting the minor axis length alters the perimeter of the crack. A larger b results in a greater perimeter, indicating a larger defect and reduced structural safety. As shown in Figure 4, an increase in b/a corresponds to a larger perimeter and higher maximum principal stress in the stress field, demonstrating that the finite element analysis results align with empirical engineering observations.

It is also evident that for the same material, the distribution of K_1 and σ_1 are similar under identical loading and boundary conditions, including the location of the maximum value that occurs at the midpoint of the crack front. Hence, given the complexity of obtaining the dynamic stress intensity factor, $K_1(t)$, for three-dimensional cracks, it is feasible to analyze $K_1(t)/K_1(0)$ using the distribution pattern of $\sigma_1(t)/\sigma_1(0)$, where $\sigma_1(t)$ is the dynamic principal stress, and $K_1(0)$ and $\sigma_1(0)$ are the static stress intensity factor and principal stress, respectively.

Table 2. Material properties of materials under examination.

Properties	Aluminum alloy	Stainless steel	Cast iron
Density (kg/m^3)	2.770	7.750	7.20
Poisson ratio	0.33	0.31	0.28
Young's Modulus (GPa)	71	193	110

Table 3. The maximum principal stress, $\sigma_{1\max}$, at the edge of crack at various angular positions for materials under examination.

Material	Angular position (θ°)	σ_{1max} (MPa)		
		$b/a = 0.25$	$b/a = 0.5$	$b/a = 0.75$
Aluminum alloy	0	3.1805	5.9523	7.8683
	45	5.9629	6.6788	7.4504
	60	5.5539	7.6166	7.1452
	90	5.4069	7.6409	7.7526
Stainless steel	0	3.1855	5.9612	7.889
	45	5.9773	6.692	7.4808
	60	5.571	7.6295	7.179
	90	5.4207	7.658	7.7813
Cast iron	0	3.1929	5.9754	7.9105
	45	5.9993	6.8662	7.5116
	60	5.5969	6.7585	7.2124
	90	5.4419	7.6852	7.8105

.

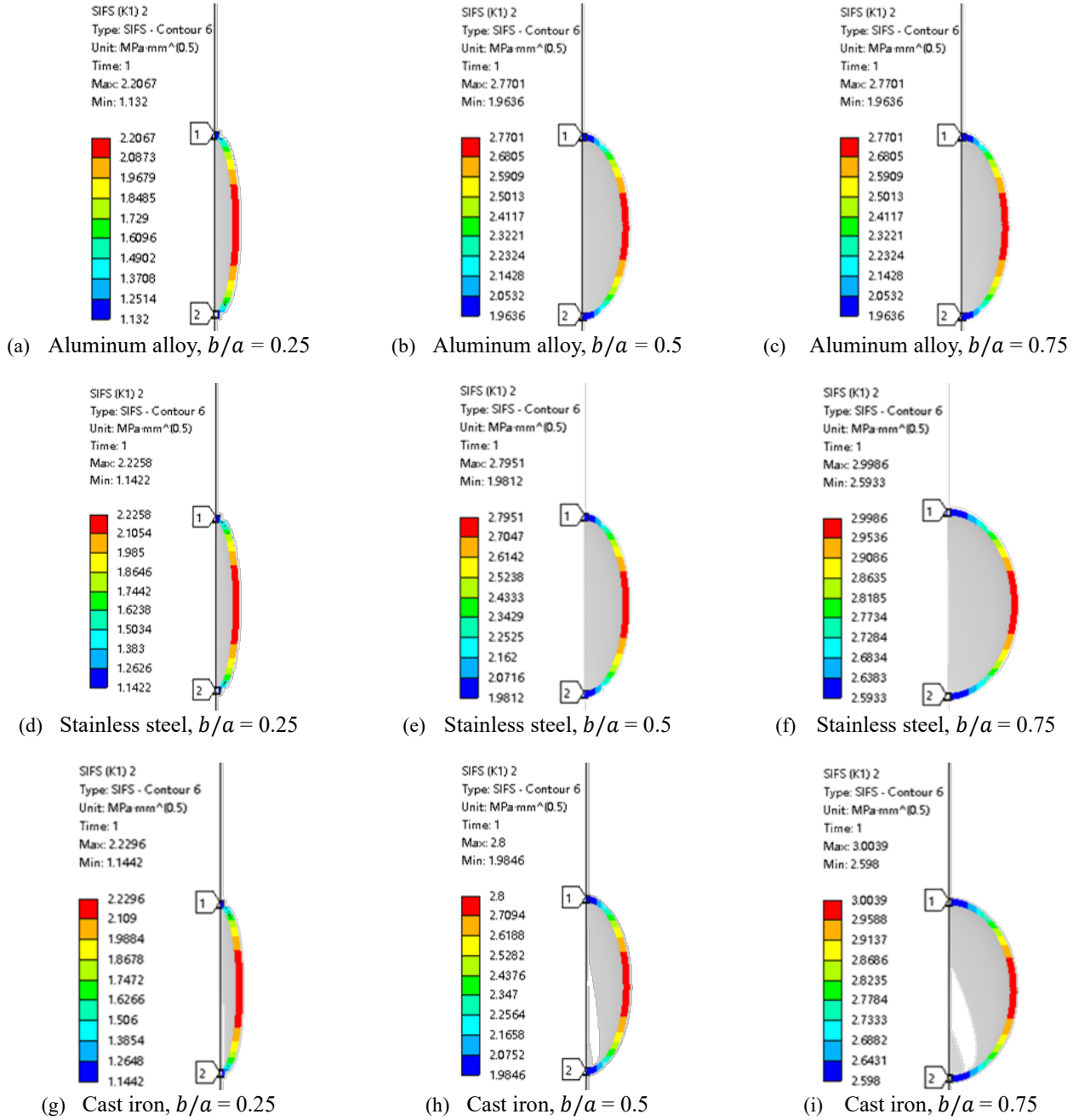

Figure 3. Stress intensity factor, K_1, at the crack front of the elliptical disc-like crack for different materials and crack shape parameter ratio, b/a.

3.3 Dynamic FEM Analysis

The dynamic analysis of the 3D elliptical disc crack under impact loading was performed using LS-DYNA. The applied impact load is given in Equation (7). The crack face is modeled using a refined tetrahedral surface mesh. As an example, the stress response of an elliptical disc crack with a long radius a = 8 mm and a short radius b = 6 mm under dynamic load for an aluminum alloy was analyzed. Figure 5 presents the stress contour of the principal stress across the cross-section of the crack front. The figures show that the stress at the crack tip is at its maximum, which is consistent with the results predicted by engineering theory. Figure 6 shows the distribution of the maximum principal stress at the front edge of the elliptical disc crack at the time when impact action is nearly finished and $\sigma_1(t)$ is get to the maximum value in material of aluminum alloy, stainless steel, and cast iron, with geometry parameters b/a is 0.25, 0.5, and 0.75, respectively. It shows that the maximum principal stress distribution is consistent well with the static analysis in Figure 4. The results indicate that the stress distribution at the leading edge of the elliptical disc crack under impact loading are influenced by both the material properties and crack geometries.

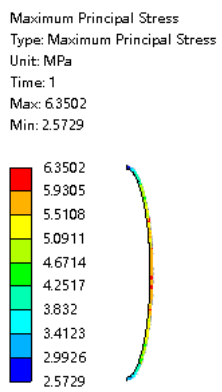

(a) Aluminum alloy, $b/a = 0.25$

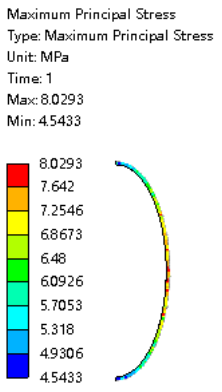

(b) Aluminum alloy, $b/a = 0.5$

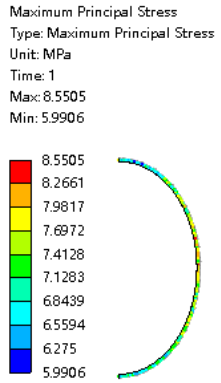

(c) Aluminum alloy, $b/a = 0.75$

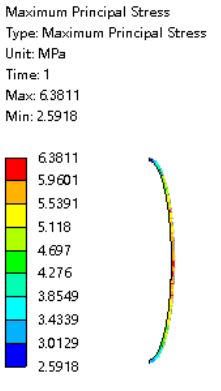

(d) Stainless steel, $b/a = 0.25$

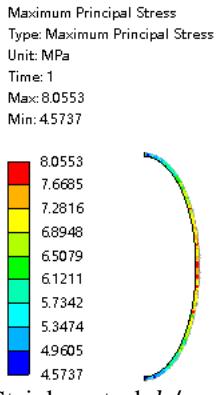

(e) Stainless steel, $b/a = 0.5$

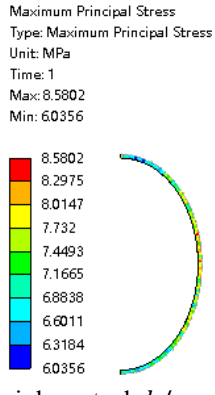

(f) Stainless steel, $b/a = 0.75$

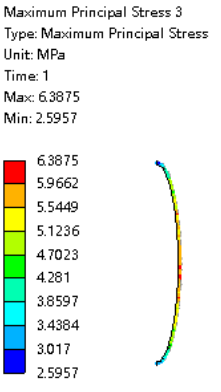

(g) Cast iron, $b/a = 0.25$

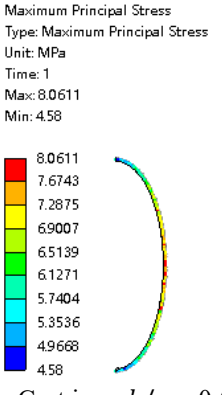

(h) Cast iron, $b/a = 0.5$

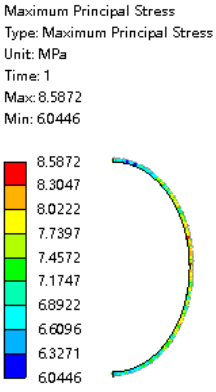

(i) Cast iron, $b/a = 0.75$

Figure 4. The maximum principal stress, $\sigma_{1\max}$, at the crack front of the elliptical disc-like crack for different materials and crack shape parameter ratios, b/a.

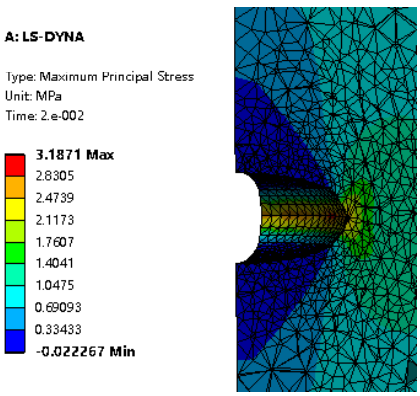

(a) σ_1 section.

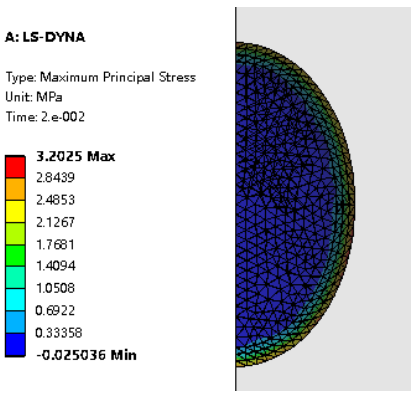

(b) σ_1 at the crack face.

Figure 5. The maximum principal stress, σ_1, at the leading edge of the elliptical disc crack under dynamic load (aluminum alloy, $a = 8$, $b = 6$).

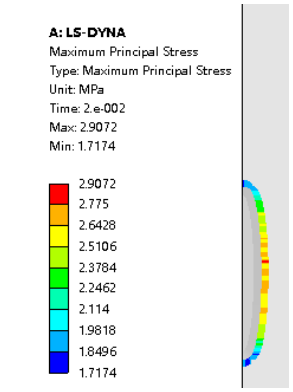

(a) Aluminum alloy, b/a = 0.25

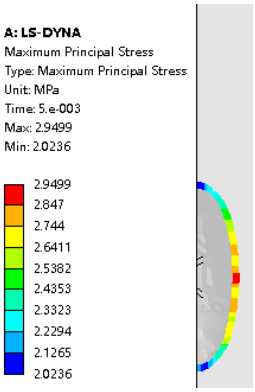

(b) Aluminum alloy, b/a = 0.5

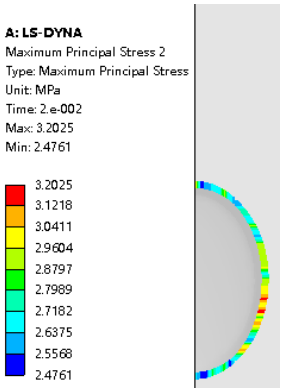

(c) Aluminum alloy, b/a = 0.75

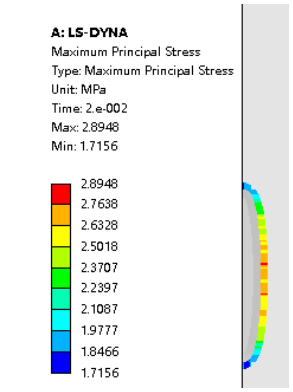

(d) Stainless steel, b/a = 0.25

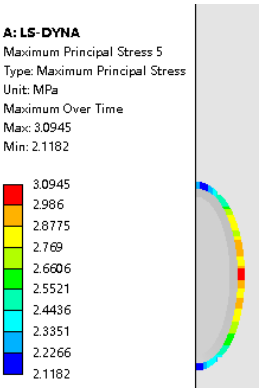

(e) Stainless steel, b/a = 0.5

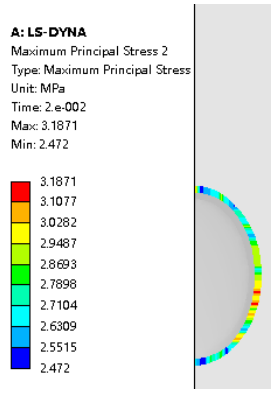

(f) Stainless steel, b/a = 0.75

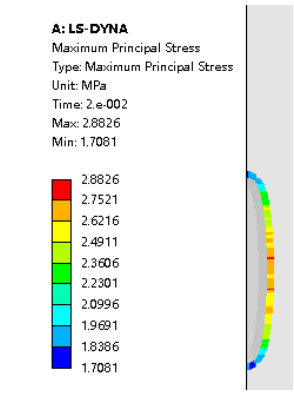

(g) Cast iron, b/a = 0.25

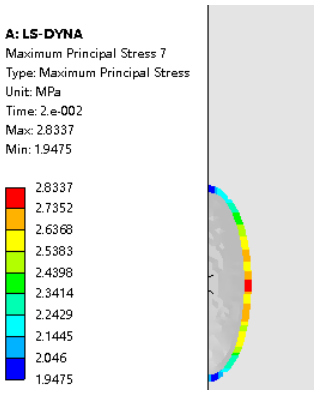

(h) Cast iron, b/a = 0.5

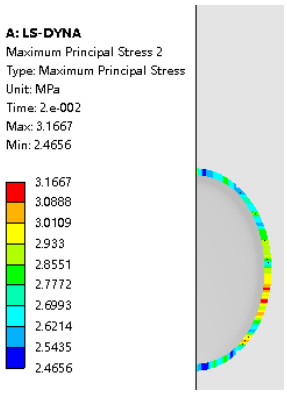

(i) Cast iron, b/a = 0.75

Figure 6. The maximum principal stress at the crack front for different materials and b/a under dynamic impact load.

The impact of the geometric parameters b/a on the principal stress of the elliptical crack with respect to the angular direction is further evaluated and presented in Figure 7. The results show that a smaller elliptical disc crack shape parameter b/a has a greater influence on the dynamic principal stress at the crack front. When b/a = 0.25, the ratio of dynamic to static principal stresses $\sigma_1(t)/\sigma_1(0)$ ranges from 0.55 to 0.72, as shown in Figures 7(a), (b), and (c). For b / a = 0.50, this ratio decreases to a range of 0.30 to 0.45. When b/a = 0.75, the ratio varies slightly for each material. These findings indicate that for the three representative engineering materials, due to stress wave propagation, the energy of the dynamic impact load dissipates within the structure, resulting in $\sigma_1(t)/\sigma_1(0) < 1$ for all cases in Figure 7. This suggests that small defects have a limited impact. Under dynamic loading, minor defects (such as micro-cracks or holes) have a negligible effect on the overall structural strength due to stress wave propagation and energy dissipation. It can be inferred that the dynamic maximum principal stress under transient impact loading is lower than the static maximum principal stress under the same loading and material conditions. Therefore, dynamic strength analysis of the leading edge of the elliptical disc crack can be effectively replaced by static fracture mechanics analysis.

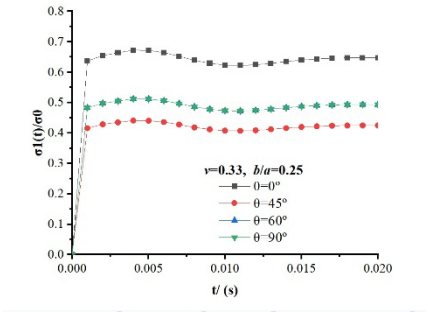

(a) Aluminum alloy, b/a = 0.25.

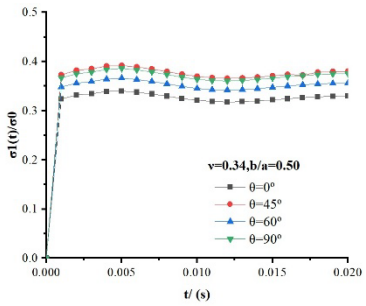

(b) Aluminum alloy, b/a = 0.5.

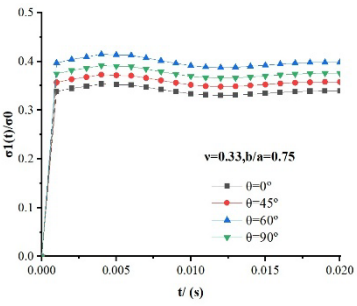

(c) Aluminum alloy, b/a = 0.75.

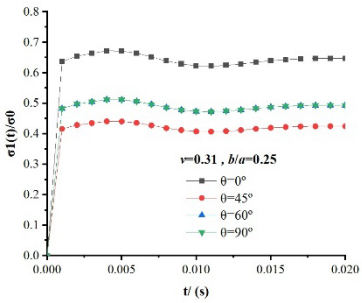

(d) Stainless steel, b/a = 0.25.

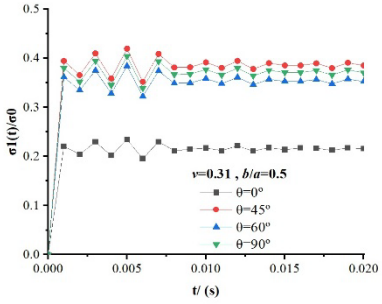

(e) Stainless steel, b/a = 0.5.

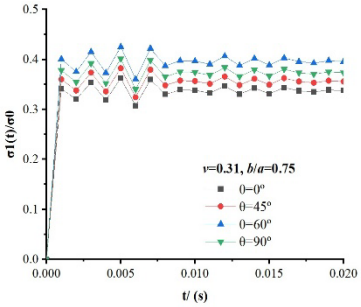

(f) Stainless steel, b/a = 0.75.

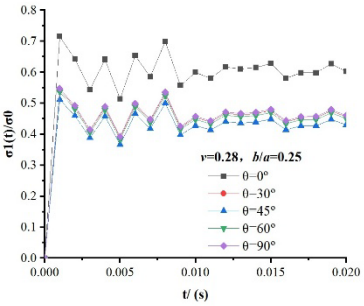

(g) Cast iron, b/a = 0.25.

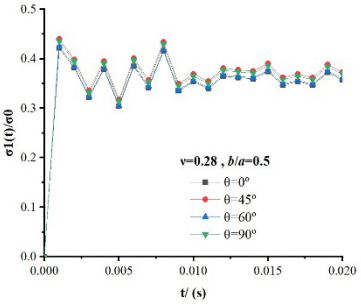

(h) Cast iron, b/a = 0.5.

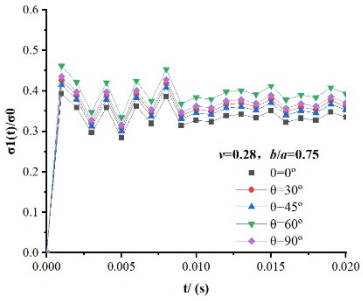

(i) Cast iron, b/a = 0.75.

Figure 7. The ratio of dynamic to static maximum principal stresses.

4. CONCLUSION

In elliptical crack analysis, analytical solutions typically consider the geometric shape parameter b/a as the primary factor influencing the stress field distribution at the crack tip. However, significant discrepancies may exist between analytical solutions and experimental results. These differences may arise due to assumptions of singularity at the crack tip in analytical models and the assumption of an infinitely large structure. In this study, the finite element method was used to analyze and compare the effects of dynamic and static loads on the stress at the crack front of a three-dimensional elliptical disc crack with different geometric shape parameters b/a in aluminum alloy, stainless steel, and cast iron. The main conclusions are as follows:

a) Although material properties influence the stress field at the crack front under both dynamic and static loading conditions, their effect is not significant when the same load and geometric shape are considered. The maximum principal stress in cast iron, which has a smaller Poisson's ratio, is slightly higher than in aluminum alloy and stainless steel, which have larger Poisson's ratios.

b) Finite element analysis under both static and dynamic conditions indicates that the geometric shape parameter b/a of the elliptical disc crack significantly affects the distribution of the maximum principal stress at the crack tip. Under the same loading conditions, a smaller b/a ratio results in a lower maximum principal stress, while a larger b/a ratio leads to a higher maximum principal stress. Since the major axis of the elliptical disc crack is assumed to be fixed, variations in b/a are achieved by altering the length of the minor axis. This change also affects the crack perimeter, where a smaller perimeter corresponds to a smaller structural defect, leading to lower maximum principal stress values. The results align with experimental findings in engineering practice.

c) Comparing dynamic and static loading conditions, the ratio of dynamic maximum principal stress to static maximum principal stress at the crack front is consistently less than 1. This indicates that under an instantaneous impact load, the maximum principal stress at the elliptical disc crack front is lower than under static loading. For three-dimensional buried elliptical cracks, the stress response at the crack front under impact loading is lower than that under static loading. Given the complexities of dynamic fracture analysis, it is feasible, under certain conditions, to replace dynamic impact load analysis with static fracture criteria for three-dimensional buried elliptical cracks.

In dynamic fracture toughness analysis of finite-sized structures, it is essential to consider not only the stress response at the crack surface and front but also the propagation of dynamic loads within the material and their interaction with the crack. These factors significantly influence crack propagation behavior. While this study focuses on impact loads, further research is required to assess the response to other forms of dynamic loading.

ACKNOWLEDGMENT AND FUNDING

The authors would like to acknowledge the support from the Ministry of Higher Education Malaysia under the Fundamental Research Grant Scheme: FRGS/1/2021/TK0/USM/02/15.

DECLARATION OF CONFLICTING INTERESTS

The authors declare no potential conflicts of interest with respect to the research and publication of this article.

REFERENCES

[1] J.W. Hutchinson, Singular behaviour at the end of a tensile crack in a hardening material, *Journal of the Mechanics of Physics of Solids*, 16, 1968, 13-31.
[2] C. Chih, On the criterion for crack extension, *Acta Metallurgica Sinica*, 13, 1977, 57-153.
[3] A. Carpinteri and M. Paggi, Asymptotic analysis in linear elasticity: From the pioneering studies by Wieghardt and Irwin until today, *Engineering Fracture Mechanics*, 76, 2009, 1771-1784.
[4] T. Adibaskoro, S. Bordas, W. T. Sołowski and S. Hostikka, Multiple discrete crack initiation and propagation in material point method, *Engineering Fracture Mechanics*, 301, 2024, 109918.
[5] A. K. Pandouria and V. Tiwari, Investigations into the static and dynamic fracture initiation and propagation toughness of AA2014-T6 incorporating temperatures effects, *Engineering Fracture Mechanics*, 281, 2023, 109136.
[6] L. B. Freund, *Dynamic Fracture Mechanics (Cambridge Monographs on Mechanics and Applied Mathematics),* Cambridge: Cambridge University Press, 1998.
[7] S. M. Nabavi and A. R. Shahani, Dynamic stress intensity factors for a longitudinal semi-elliptical crack in a thick-walled cylinder, *International Journal of Engineering, Science and Technology*, 6, 2014, 57-77.
[8] Z. Zhang, H. Wang, L. Zhong and L. Tang, Experimental and numerical research of the behavior of 3D internal cracks under uniaxial compression using 3D-ILC technology, *Theoretical and Applied Fracture Mechanics*, 124, 2023, 103819.
[9] D. He, Z. Guo, H. Ma and T. Li, Single high-order smooth element for simulating flat internal elliptical cracks, *Theoretical and Applied Fracture Mechanics*, 136, 2025, 104838.
[10] T. L. Anderson, Fracture mechanics: fundamentals and applications, Boca Raton: CRC Press, 1991.
[11] C. Zhang, R. Sun, J. Yin, Y. Hu, Q. Dou, Z. Tang, Y. Miao and Y. Li, Failure behaviours of steel/aluminium threaded connections under impact fatigue, *Engineering Failure Analysis*, 174, 2025, 109473.
[12] F. Tianyou, *Theoretical Basis of Fracture,* Beijing: Science Press, 2003.
[13] A. E. Green and I. N. Snedddon, The distribution of stress in the neighbourhood of a flat elliptical crack in an elastic solid, *Proceedings of the Cambridge Philosophical Society*, 46, 1950, 159-163.
[14] Y. J. Guo and J. A. Nairn. Three-dimensional dynamic fracture analysis using the material point method, *Computer Modeling in Engineering and Sciences,* 16, 2006, 141-155.
[15] Y. Wang, D. Xing, M. Yu and Q. Qiao, Experimental study of internal deformation in 3D solids with embedded parallel cracks during the fracture process using multi-material 3D printing and stereo digital image correlation, *Theoretical and Applied Fracture Mechanics*, 137, 2025, 104884.
[16] F. Gálvez, D. Cendón, N. García, A. Enfedaque and V. Sánchez-Gálvez. Dynamic fracture toughness of a high strength armor steel, *Engineering Failure Analysis*, 16(8), 2009, 2567-2575.